LRP 412/90 September 1990

EQUILIBRIUM GRADIENT EFFECTS IN THE THEORY OF ALFVEN WAVE HEATING

A. Jaun, J. Vaclavik and K. Appert

submitted for publication in

Plasma Physics and Controlled Fusion

Equilibrium Gradient Effects in the Theory of Alfven Wave Heating

A. Jaun, J. Vaclavik and K.Appert

Centre de Recherches en Physique des Plasmas
Association Euratom - Confédération Suisse
Ecole Polytechnique Fédérale de Lausanne
21, av. des Bains – CH-1007 Lausanne/Switzerland

September 4, 1990

Abstract

An explicit expression for the local power absorption density in a uniformly magnetized slab plasma is derived from the Vlasov-Maxwell equations, taking into account density and temperature gradients. Using a transformation to lagrangian coordinates, the kinetic flux of energy due to particle streaming can be separated in a unique way from the actual power dissipation.

Computations using this expression show how equilibrium gradients play a role in the modelling of low-frequency Alfven wave heating, and give a threshold below which the gradient effects are important in a medium size tokamak.

1 Introduction

The absorption of waves in non uniform plasmas is one of the principal problems in the theory of radio frequency heating. Of particular interest is the determination of the power absorption density per species as a function of suitable spatial coordinates. Recently a general formulation for the local power absorption density has been obtained from the Vlasov equation assuming a locally homogeneous plasma (Vaclavik and Appert, 1987). Such a formulation has been needed to guarantee positive power deposition profiles all over the plasma.

In low frequency regimes, effects due to temperature and density gradients become important, and may even lead to instabilities. Homogeneity may then not be assumed any longer when calculating power profiles. This naturally leads to questions about the threshold below which gradients significantly contribute, and how they do.

In the present work, we study these gradient effects on the modelling of Alfven wave heating. We first derive an expression for the local power absorption density assuming a hot, uniformly magnetized, inhomogeneous plasma. Using a 1-D finite element, full wave code, the power deposition is computed for low frequency Alfven waves in a plasma with parabolic density and temperature profiles. A threshold is given beyond which we show that gradient effects become important.

2 Power Deposition

In this section we derive an expression for the local power absorption density of a small amplitude eletromagnetic field in a hot, uniformly magnetized, inhomogeneous plasma.

Using a transformation to Lagrangian coordinates, the power is calculated without introducing the flux due to particle streaming, and corresponds to the local exchange of energy between the wave and the particles. This technique was found necessary to guarantee positive absorption profiles in homogeneous plasmas, which are known to be stable.

The derivation is along the same lines as for the homogeneous case, except that now effects due to density and temperature gradients are included. The energy moment of the Vlasov equation is first transformed into Lagrangian coordinates. A time averaging over the scale $\Delta\tau \sim |\omega - \Omega_c|^{-1}$ where ω is the excitation frequency and Ω_c the cyclotron frequency of the species, must be carried out concurrently with an averaging in space over $\lambda_\parallel = \Delta\tau v_\parallel$ the distance a particle with a typical velocity component $v_\parallel$ along the equilibrium magnetic field $\boldsymbol{B}_o$ travels during the time $\Delta\tau$. Doing so, we obtain a general expression for the local power absorption density as

$$P_L(\boldsymbol{x}_\perp) = \frac{q}{2}\int d\boldsymbol{v}\; Re < \boldsymbol{E}^*(\boldsymbol{x}'_\perp)\cdot \boldsymbol{v}' f_1(\boldsymbol{x}'_\perp, \boldsymbol{v}') >_{t'} \tag{1}$$

where we have set

$$f = f_0 + f_1 + \mathcal{O}(\boldsymbol{E}^2), \tag{2}$$

$$\{\boldsymbol{E}(\boldsymbol{x},t), f_1(\boldsymbol{x},\boldsymbol{v},t)\} = Re\,\{\boldsymbol{E}(\boldsymbol{x}_\perp), f_1(\boldsymbol{x}_\perp,\boldsymbol{v})\}\exp[i(k_\parallel x_\parallel - \omega t)]. \tag{3}$$

Here f is the distribution function of a species with charge q and mass m, while f_1 is the linear perturbation induced in the presence of the electromagnetic field $\boldsymbol{E}$ and $\boldsymbol{B}$. Primed quantities $\boldsymbol{x}'$,$\boldsymbol{v}'$,t' refer to position, velocity and time in the Lagrangian frame of reference with the trajectories of particles given by

$$\begin{aligned}
&\boldsymbol{x}'_\perp = \boldsymbol{x}_\perp + \frac{v_\perp}{\Omega_c}\left[(\sin\alpha - \sin\alpha')\boldsymbol{e}_x + (\cos\alpha' - \cos\alpha)\boldsymbol{e}_y\right],\\
&\boldsymbol{v}' = v_\perp(\cos\alpha'\boldsymbol{e}_x + \sin\alpha'\boldsymbol{e}_y) + v_z\boldsymbol{e}_z,\\
&\alpha' = \alpha + \Omega_c(t - t'), \quad v_\perp = (v_x^2 + v_y^2)^{1/2}, \quad \alpha = \tan\frac{v_y}{v_x}
\end{aligned} \tag{4}$$

The cartesian coordinate system was chosen with the z-axis along the static magnetic field $\boldsymbol{B}_o$. It is interesting to note here, that the trajectories of particles depend exclusively on $\boldsymbol{B}_o$, and are the same whether homogeneity is assumed or not. The only term in (1) carrying information about the inhomogeneity is $f_1(\boldsymbol{x}'_\perp, \boldsymbol{v}')$

Next, by integrating the Vlasov equation over unperturbed orbits, f_1 is related to the equilibrium distribution function f_0, which is known to have a dependency of the form $f_0(X = x + v_y/\Omega_c, Y = y - v_x/\Omega_c, v_\parallel, v_\perp)$, all four parameters being constants of

motion. For practical use, f_0 is assumed maxwellian

$$f_0(\boldsymbol{X}_\perp, v_\perp, v_\parallel) \equiv f_M = \pi^{-3/2}\, n_0\, v_t^{-3} \exp\left[-\frac{(v_\perp^2 + v_\parallel^2)}{v_t^2}\right], \qquad v_t = \left(\frac{2T}{m}\right)^{1/2} \tag{5}$$

where $n_0(\boldsymbol{X}_\perp)$ and $T(\boldsymbol{X}_\perp)$ are the plasma density and temperature. Upon using the Fourier transforms

$$\{\boldsymbol{E}(\boldsymbol{x}_\perp), f_1(\boldsymbol{x}_\perp, \boldsymbol{v})\} = \int d\boldsymbol{k}_\perp \exp\left[i(\boldsymbol{k}_\perp \cdot \boldsymbol{x}_\perp)\right] \{\boldsymbol{E}(\boldsymbol{k}_\perp), f_1(\boldsymbol{k}_\perp, \boldsymbol{v})\} \tag{6}$$

$$f_0(\boldsymbol{X}_\perp, \boldsymbol{v}) = \int d\boldsymbol{q}_\perp \exp\left[iq_x(x + v_y/\Omega_c)\right] \exp\left[iq_y(y - v_x/\Omega_c)\right] f_0(\boldsymbol{q}_\perp, v_\perp, v_\parallel) \tag{7}$$

we obtain

$$\begin{aligned} f_1(\boldsymbol{k}, \boldsymbol{v}, \omega) \;=\; & \exp\left[\frac{i}{\Omega_c}(\boldsymbol{k} \times \boldsymbol{v}) \cdot \boldsymbol{e}_z\right] \sum_\ell \exp[-i\ell\alpha] \\ & \times \int d\boldsymbol{q}_\perp \exp[i\ell\varphi_{k-q}]\, \frac{-iq/m}{(\omega - k_\parallel v_\parallel - \ell\Omega_c)} \\ & \times \boldsymbol{A}_\ell(\boldsymbol{k}, \boldsymbol{q}_\perp, v_\perp, v_\parallel, \omega) \cdot \boldsymbol{E}(\boldsymbol{k}_\perp - \boldsymbol{q}_\perp) \end{aligned} \tag{8}$$

$$\begin{aligned} A_{\ell,x} \;=\; & \left\{\left(\frac{-2v_\perp}{v_t^2}\right)\left[\frac{\ell}{\Delta\xi} J_\ell(\Delta\xi)\cos(\varphi_{k-q}) - iJ_\ell'(\Delta\xi)\sin(\varphi_{k-q})\right]\right. \\ & + \frac{i}{\Omega_c} J_\ell(\Delta\xi)\left[\frac{k_\parallel v_\parallel}{\omega} - 1\right] q_y \\ & + i\left[q_y \sin(\varphi_{k-q}) + q_x \cos(\varphi_{k-q})\right] \frac{\ell}{\omega} J_\ell(\Delta\xi)\sin(\varphi_{k-q}) \\ & \left. + i\left[q_y \cos(\varphi_{k-q}) - q_x \sin(\varphi_{k-q})\right] i\frac{\Delta\xi}{\omega} J_\ell'(\Delta\xi)\sin(\varphi_{k-q})\right\} f_M \end{aligned} \tag{9}$$

$$\begin{aligned} A_{\ell,y} \;=\; & \left\{\left(\frac{-2v_\perp}{v_t^2}\right)\left[\frac{\ell}{\Delta\xi} J_\ell(\Delta\xi)\sin(\varphi_{k-q}) + iJ_\ell'(\Delta\xi)\cos(\varphi_{k-q})\right]\right. \\ & - \frac{i}{\Omega_c} J_\ell(\Delta\xi)\left[\frac{k_\parallel v_\parallel}{\omega} - 1\right] q_x \\ & - i\left[q_y \sin(\varphi_{k-q}) + q_x \cos(\varphi_{k-q})\right] \frac{\ell}{\omega} J_\ell(\Delta\xi)\cos(\varphi_{k-q}) \\ & \left. - i\left[q_y \cos(\varphi_{k-q}) - q_x \sin(\varphi_{k-q})\right] i\frac{\Delta\xi}{\omega} J_\ell'(\Delta\xi)\cos(\varphi_{k-q})\right\} f_M \end{aligned} \tag{10}$$

$$\begin{aligned} A_{\ell,z} \;=\; & \left\{\left(\frac{-2v_\parallel}{v_t^2}\right) J_\ell(\Delta\xi)\right. \\ & \left. - i\left[q_y \cos(\varphi_{k-q}) - q_x \sin(\varphi_{k-q})\right]\left[\frac{|\boldsymbol{k}_\perp - \boldsymbol{q}_\perp| v_\parallel}{\omega\Omega_c}\right] J_\ell(\Delta\xi)\right\} f_M \end{aligned} \tag{11}$$

$$\Delta\xi = \frac{v_\perp}{\Omega_c}|\boldsymbol{k}_\perp - \boldsymbol{q}_\perp|, \qquad \tan\varphi_{k-q} = \left(\frac{k_y - q_y}{k_x - q_x}\right) \tag{12}$$

which is equivalent to a similar expression derived by Yasseen and Vaclavik (1986) using an another method. J_ℓ and J'_ℓ represent respectively are the Bessel function and its derivative. In order to satisfy causality, the frequency ω is assumed to have a small, positive, imaginary part.

A general form of the local power absorption density may now be obtained by inserting (4) and (8) into (1) and carrying out the time averaging. For practical use however, we restrict ourselves to the case where the Larmor radii of the species are small when compared first to the scale of variation of the electric field and secondly to the equilibrium parameters such as temperature and density. Assuming homogeneity in one direction across $\boldsymbol{B}_0$ allows us to treat y as an ignorable coordinate of the equilibrium. Some rearrangements finally yield an expression for local power absorption in slab geometry, valid up to second order in the equilibrium and field gradients:

$$\begin{aligned} P_L \;=\; & P_{hom} \;+ \\ & \frac{1}{8\pi}\Bigg\{\left(\frac{\omega}{k_\parallel\Omega_c}\right)^2\left[\tfrac{1}{2}|E_z|^2\frac{d^2}{dx^2} + \left(\frac{d}{dx}|E_z|^2\right)\frac{d}{dx}\right]\tilde{Y}_0 \;-\; \left(\frac{\omega k_y}{\Omega_c k_\parallel^2}\right)|E_z|^2\frac{d}{dx}\tilde{Y}_0 \\ & \quad + \left[\tfrac{1}{2}|E_+|^2\frac{d^2}{dx^2} + \left(\frac{d}{dx}|E_+|^2\right)\frac{d}{dx}\right]\rho_L^2\tilde{Y}_1 \;-\; \left(\frac{k_y}{2\omega\Omega_c}\right)|E_+|^2\frac{d}{dx}Y_1 \\ & \quad + \left[\tfrac{1}{2}|E_-|^2\frac{d^2}{dx^2} + \left(\frac{d}{dx}|E_-|^2\right)\frac{d}{dx}\right]\rho_L^2\tilde{Y}_{-1} - \left(\frac{k_y}{2\omega\Omega_c}\right)|E_-|^2\frac{d}{dx}Y_{-1}\Bigg\} \end{aligned} \tag{13}$$

$$\begin{aligned} & E_\pm = (E_x \pm iE_y), \qquad \rho_L = \left(\frac{T}{m\Omega_c^2}\right)^{1/2} \\ & \tilde{Y}_\ell = \frac{\omega_p^2}{(\omega - \ell\Omega_c)}Y_\ell^S, \qquad Y_\ell = \frac{T}{m}\tilde{Y}_\ell, \qquad Y_\ell^S = Y^S\left(\frac{\omega - \ell\Omega_c}{|k_\parallel|v_t}\right). \end{aligned} \tag{14}$$

P_{hom} refers to the absorption in the homogeneous case as found by Vaclavik and Appert (1987), and Y^S is the imaginary part of the plasma dispersion function as defined by Shafranov (1967).

To conclude this section, we write the time averaged Poynting theorem as

$$\frac{dS}{dx} = -\frac{\omega}{8\pi}Im(\boldsymbol{E}^* \cdot \boldsymbol{\epsilon} \cdot \boldsymbol{E}) \tag{15}$$

where S is the time averaged x-component of the Poynting vector and ϵ the dielectric tensor of the plasma as derived by Martin and Vaclavik (1987). The rhs of Eq. (15) consists of dissipative terms P_L and energy flux terms S_T due to thermal motion of particles. Taking the difference

$$-\frac{\omega}{8\pi} Im(\boldsymbol{E}^* \cdot \epsilon \cdot \boldsymbol{E}) - P_L = \frac{dS_T}{dx} \tag{16}$$

both contributions P_L and $\frac{dS_T}{dx}$ are separated in a unique way.

3 Numerical Results

The expression for local power absorption obtained in the previous section, together with an expression for the dielectric tensor derived by Martin and Vaclavik (1987) can now be used to study numerically the effects of density and temperature gradients on the excitation of Alfven waves in a medium size tokamak. Since these effects are found to be stronger at low frequencies, we concentrate on this part of the spectrum.

The eigenmode equation

$$\nabla \times \nabla \times \boldsymbol{E} = \frac{\omega^2}{c^2} \epsilon \cdot \boldsymbol{E}, \qquad \boldsymbol{E} \sim \exp(-i\omega t) \tag{17}$$

is solved for a plasma slab, using the cubic-hermite finite element code ISMENE (Appert *et al.*, 1986; Appert *et al.*, 1987). The parameters used for the computations, unless otherwise specified, are those of a medium size tokamak (TCA) (Collins *et al.*, 1986) and are summarized in Table 1. The density and temperature profiles of the deuterium plasma are

$$n(x) = n_0 \left(1 - s\frac{x^2}{a^2}\right), \qquad T_{e,i}(x) = T_{i0,e0} \left(1 - s\frac{x^2}{a^2}\right)^2 \tag{18}$$

while the axial wave number k_z was chosen to obtain several Alfven oscillations within the plasma. The calculation was discretized on an irregular mesh of 400 points, with a higher density of points around the boundaries.

Static magnetic field	B_0	$[kG]$	15
Minor radius	a	$[cm]$	18
Central density	n_0	$[cm^3]$	2.3×10^{13}
Central ion temperature	T_{i0}	$[eV]$	350
Central electron temperature	T_{e0}	$[eV]$	800
Profile shape factor (Eq. 18)	s		0.95
Poloidal wave number	k_y	$[cm^{-1}]$	-5.0×10^{-2}
Axial wave number	k_z	$[cm^{-1}]$	5.6×10^{-3}
Frequency	f_0	$[kHz]$	500

Table 1: Default computation parameters

Shown in Fig. 1, are the waveforms for the case where a fast magnetosonic surface wave mode converts into a kinetic Alfven wave. For this, we recognise a typical conversion pattern: the antenna, which is situated outside the plasma at $x_{ant} = 19$ cm, between the wall at $x_{wall} = 21$ cm and the plasma edge at $x_{plasma} = 18$ cm, first couples to the fast magnetosonic cut-off wave, which is not apparent in the figure. Around $x = 8$ cm, it meets the Alfven spatial resonance and converts into a kinetic Alfven wave (KAW). This then propagates inwards to higher density regions and builds up a standing wave (global eigenmodes of the KAW) if it is not damped out before it reaches the center. Near the edge, where the temperature is sufficiently low to have $k_z v_{te} < \omega$, the short wavelength oscillation can be identified as the surface quasi-electrostatic wave (SQEW) directly excited by the antenna.

Let us now analyse the effect of equilibrium gradients on the electric field (Figs. 1 and 2) and on the corresponding local power deposition profiles (Figs. 3 and 4). At 2.5 MHz, the waveform is essentially the same as for the calculation made without equilibrium gradient terms and the amplitude is changed by less than 5%. In contrast, the field structure is clearly affected by the gradients on the antenna side from 1 MHz downwards. The corresponding absorption profile (Fig. 4b) shows that they remove a false peak near $x = 16$ cm, which grows as the frequency decreases. Below 250 kHz, the difference is so great that the fields and absorption profiles become meaningless if

the gradients are not taken into account.

Important for consistency, and as a check for the previously derived expression, is to ensure that the power radiated by the antenna

$$P_{ant} = -\frac{1}{2} Re \int_{vacuum} d^3x \; \boldsymbol{j}_{ant} \cdot \boldsymbol{E}^* \tag{19}$$

where $\boldsymbol{j}_{ant}$ denotes the antenna current, equal to the local power absorption (13) integrated all over the plasma volume. While this is clearly wrong for low frequencies if equilibrium gradients are neglected, very good agreement (up to 3 digits) has been obtained using the full expression.

As a first conclusion, we see that the threshold beyond which gradients are qualitatively affecting the fields and the absorption profiles, lies around 1 MHz. Surprisingly, the effect on the electric field is more to maintain the high frequency wave structure down below the threshold rather than to modify it. Except for the amplitudes which decrease as a power of the excitation frequency, the field and absorption profiles obtained using the full expressions change little over the whole frequency range studied here.

Having examined local properties, we now concentrate on a more global approach where only the total amount of absorbed power all over the plasma is taken into account (Figs. 5 and 6). With increasing ω/k_z, the absorption suddenly peaks when the resonance condition $\omega/k_z = c_A$ is met in the center of the plasma. Standing waves (KAW) appear between the resonance layers. This results in small peaks of the total absorption around $\omega/k_z = 5 \times 10^8 [cm/s]$, one for each new higher order mode, when the resonance layers move towards the outside to lower density regions. Before ω/k_z has become too much larger, strong damping keeps the kinetic Alfven wave from reaching the center of the plasma preventing any further build up of standing waves. The total power then remains constant over the whole range called the Alfven continuum (CONT), where the wave is absorbed within a short distance of the resonance point. The peaks in total power at high phase velocity ($\omega/k_z > 8 \times 10^8 [cm/s]$) are related to

the eigenmodes of the cold SQEW wave. Starting from a high value of the parameter ω/k_z, the computations show first a peak in the absorption when the fundamental is built up at the edge ($\omega/k_z \simeq 1.06 \times 10^9 [cm/s]$ for 2.5 MHz), while other peaks are found for higher order modes if one keeps decreasing ω/k_z. It is important here to note that even though the effects of the KAW and SQEW waves on the total power absorption are well separated in phase velocities, both may coexist in the same plasma, one effect simply dominating the other in a certain regime.

Fig. 5 shows how quickly the total absorption decreases with the frequency (almost as its fifth power). The wave scenario which has just been described however remains essentially unchanged down to 25 kHz. This seems to indicate that the power decrease is mainly due to a drop in the coupling between the antenna and the cut-off field which carries the energy to the resonance.

Finally, a comparison of Fig. 5 and 6 shows the effect of the equilibrium gradients on the total absorption. As expected, their contribution increases for small frequencies, the general tendency being to overestimate the absorbed power if the gradients are neglected. With a frequency of 2.5 MHz, the total absorption is almost insensitive to their presence, except for the phase velocities below the Alfven resonance and for the fundamental SQEW mode, where the discrepancies are of the order of a factor 10. Below 500 kHz however, the power step due to the Alfven resonance disappears if gradients are neglected and the higher order SQEW modes are ill represented. The least affected is certainly the Alfven continuum (CONT) where the corrections are less than a factor of two over the whole range of frequencies. It is however important to keep in mind that although the corrections are weak if the power absorption is integrated over the whole plasma, the deposition profile on which the total is based is completely wrong for low frequencies.

To summarize, gradient terms, as in the local analysis again remove deviations from the well known pattern at high frequencies which would have appeared below approximatively 1 MHz if they had been neglected. The step in power due to the

Alfven resonance and the peaks of power due to the SQEW modes survive down to 50 kHz.

4 Conclusion

An analytical expression for the local power absorption density in a uniformly magnetized, inhomogeneous slab plasma has been derived and successfully implemented in a computer code, showing good agreement with the total power emitted on the antenna.

Applied to the tokamak of our laboratory, computations in the Alfven range of frequencies showed that below 1 MHz, equilibrium gradients become important. Taken into account, the usual conversion scenario remains valid down to frequencies below 100 kHz, although the absorbed power and the electric field quickly decrease in amplitude with the applied frequency. Neglected, the waveforms become deficient on the antenna side and the total absorption is overestimated by several orders of magnitude.

5 Acknowledgement

The authors whish to thank Dr. R. Parker for reading the manuscript. This work was supported in part by the Swiss National Science Foundation.

References

Appert K., Hellsten T., Vaclavik J., Villard L., *Comput. Phys. Commun.* **40** (1986) 73.

Appert K., Hellsten T. Lütjens H., Sauter O., Vaclavik J., Villard L. in *Proc. 7th Int. Conf. on Plasma Physics*, Kiev, Invited Papers **Vol.2** (1987) 1230.

Martin Th., Vaclavik J., *Helv. Phys. Acta* **60** (1987) 471.

Shafranov V.D. in Reviews of Plasma Physics, edited by M.A. Leontovich (Consultants Bureau, New York, 1967) Vol. **3**

Vaclavik J., Appert K., *Plasma Phys. and Contr. Fusion* **29** (1987) 257.

Yasseen F., Vaclavik J., *Phys. Fluids* **29** (1986) 450.

Collins G.A. *et al.*, Phys. Fluids **29**, (1986) 2260 and references cited therein.

Figure Caption

Figure 1: Parallel electric fields, including equilibrium gradients

Figure 2: Parallel electric fields, neglecting equilibrium gradients

Figure 3: Power deposition profiles, including equilibrium gradients

Figure 4: Power deposition profiles, neglecting equilibrium gradients

Figure 5: Total power absorption, including equilibrium gradients

Figure 6: Total power absorption, neglecting equilibrium gradients

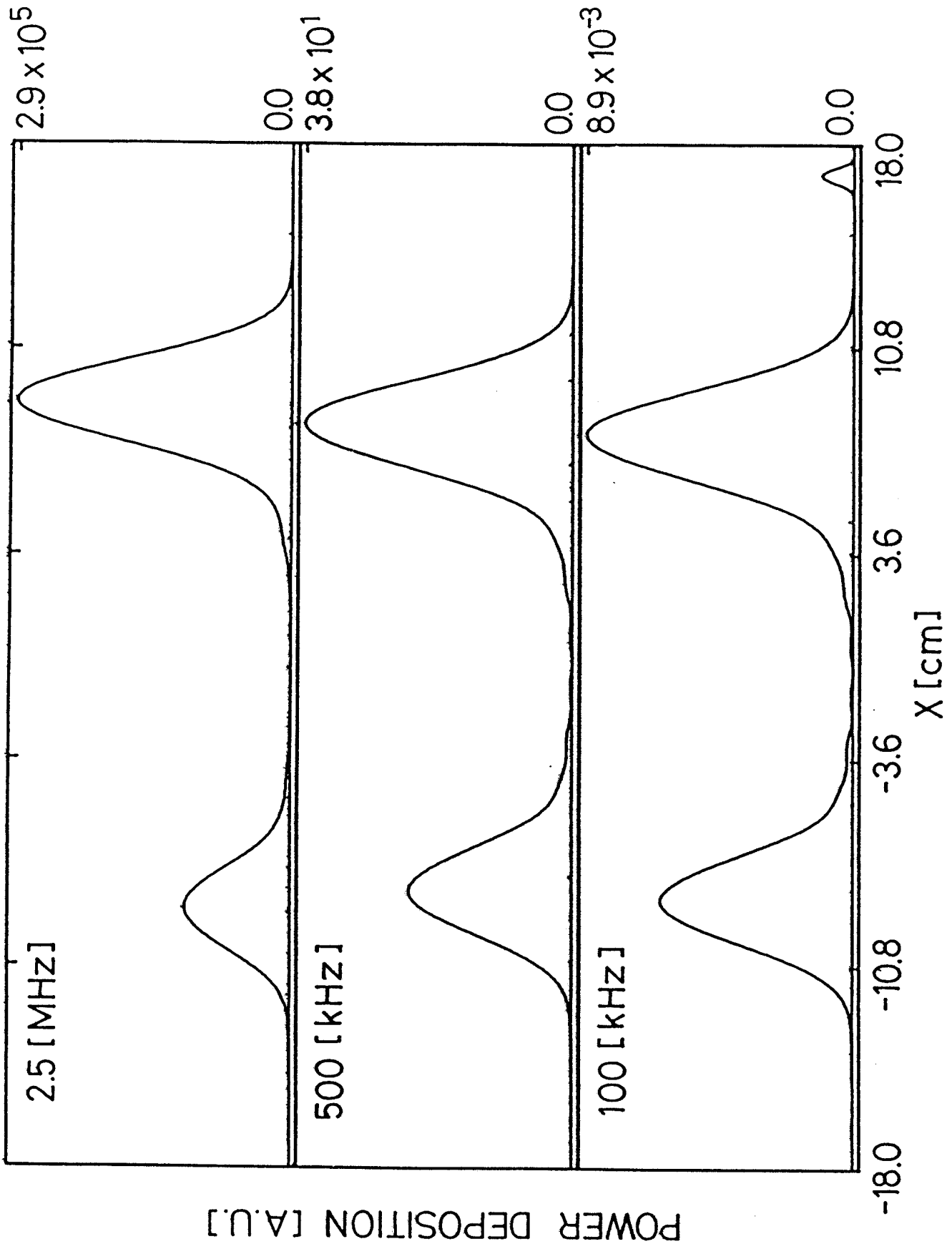

Figure 3: Power deposition profiles, including equilibrium gradients

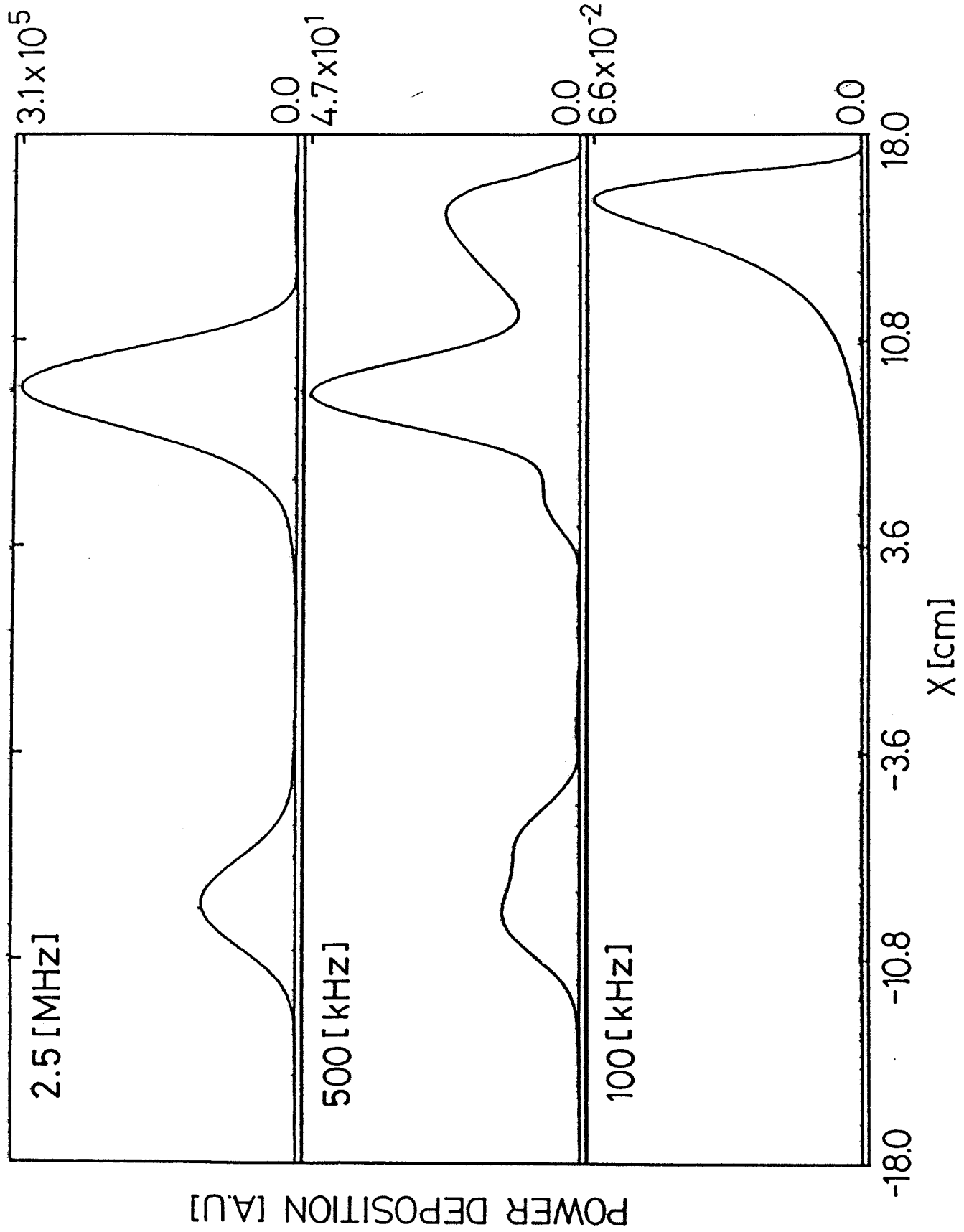

Figure 4: Power deposition profiles, neglecting equilibrium gradients

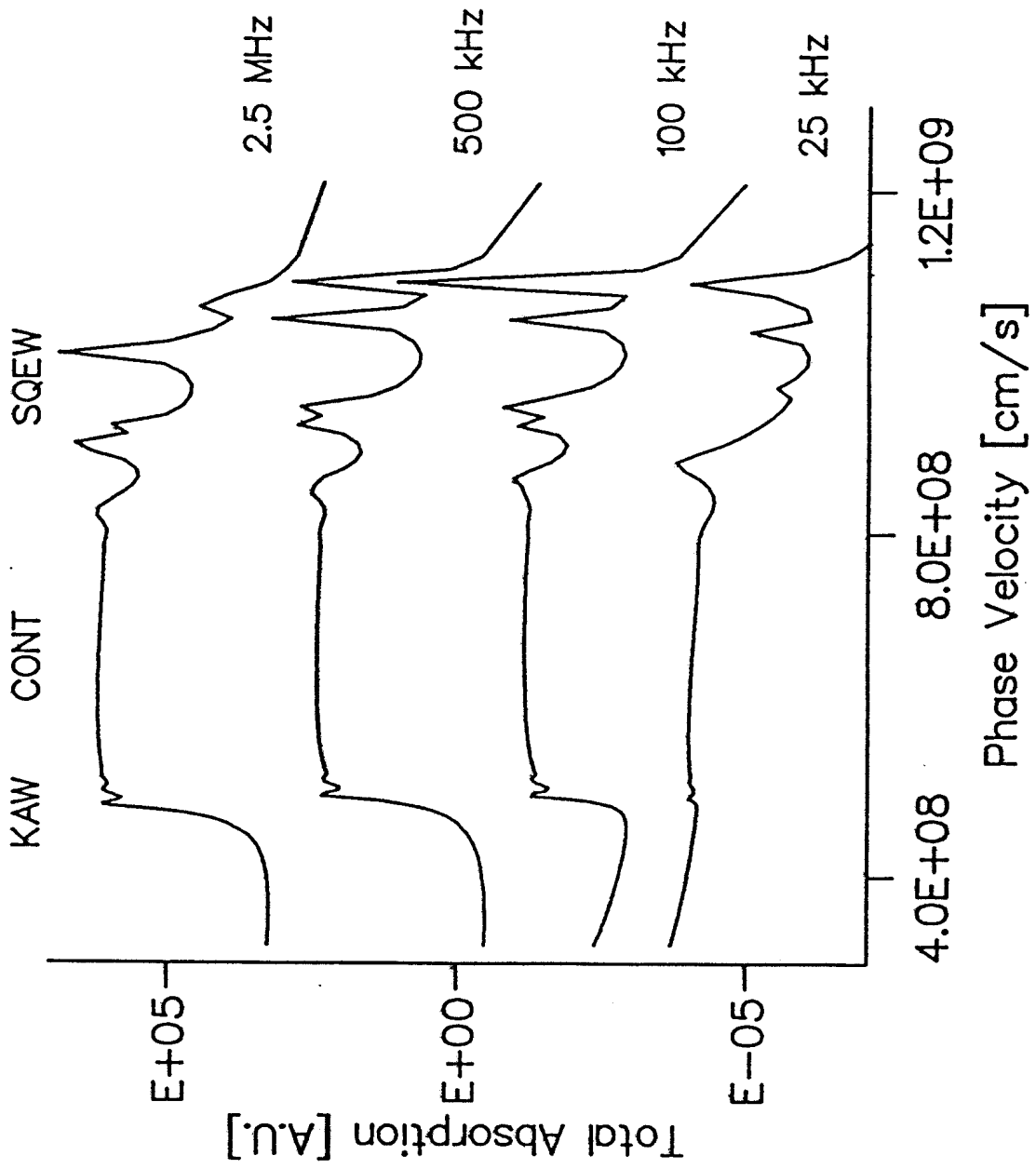

Figure 5: Total power absorption, including equilibrium gradients

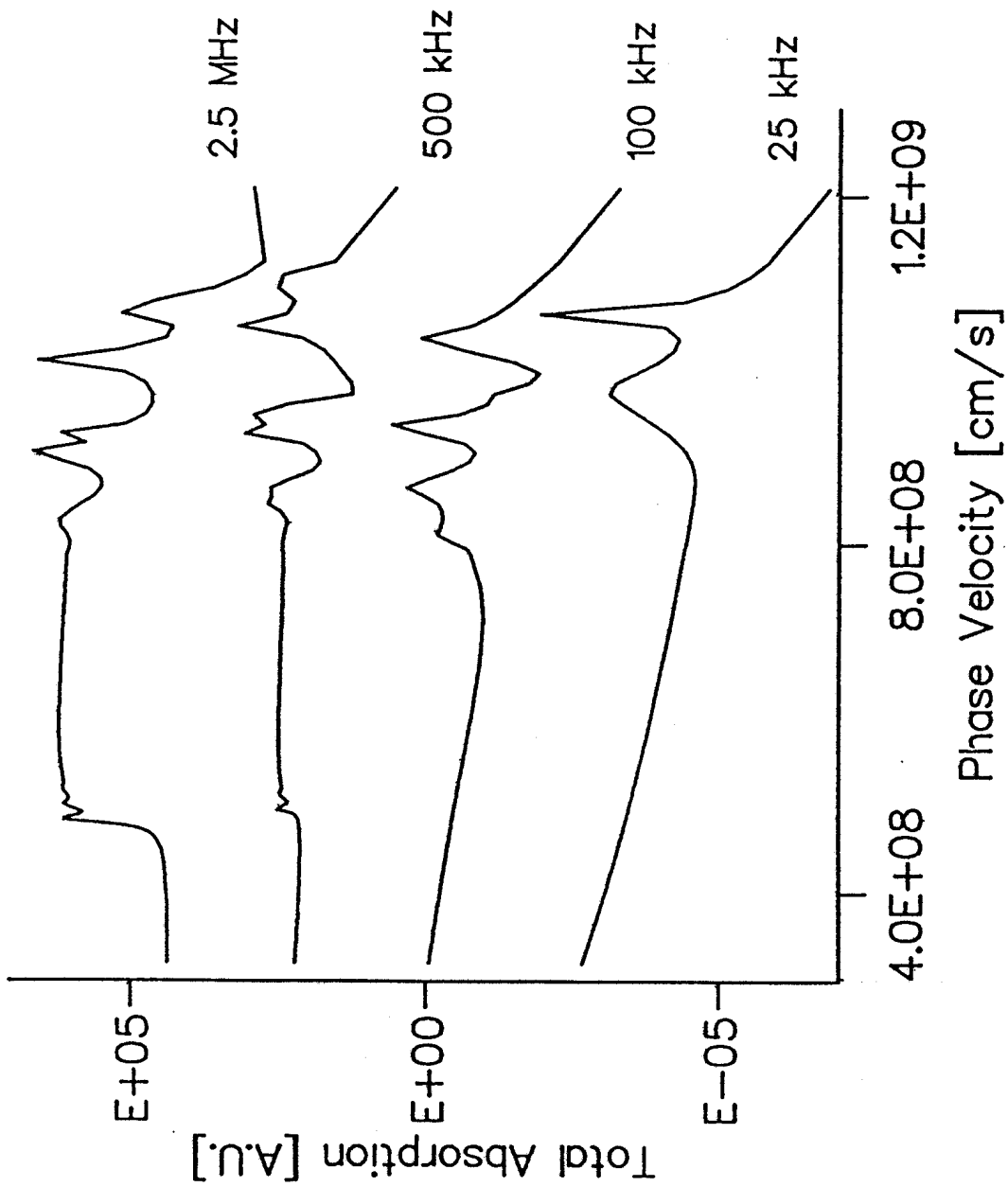

Figure 6: Total power absorption, neglecting equilibrium gradients